

Wit GRZESIK<sup>1</sup>  
Krzysztof ZAK<sup>1</sup>  
Mariusz PRAZMOWSKI<sup>1</sup>

## **SURFACE INTEGRITY OF HARD TURNED PARTS MODIFIED BY BALL BURNISHING**

The purpose of this research is to test the applicability of ball burnishing for improving surface integrity produced in hard machining on parts made of high-strength, low alloy 41Cr4 steel with hardness of about 57 HRC. Machined surfaces were characterized using 2D and 3D scanning techniques. Moreover, the distribution of microhardness beneath the surface was determined and the microstructure of the sublayer was examined using SEM/EDS technique. This investigation confirms that ball burnishing allows producing surfaces with acceptable surface roughness and better service properties. The main conclusion is that this sequential technology can partly eliminate grinding operations when hard machining is not enough to produce the desired surface integrity.

### **1. INTRODUCTION**

Machining of hardened materials, mainly steels, is one of the leading removal method of producing parts in such manufacturing branches as automotive, bearing, hydraulic and die and mold making sectors [1]. However, this technology has several drawbacks in comparison to grinding operations including lower surface finish and unsatisfactory dimensional accuracy [2]. In consequence, hard turned surfaces should be additionally finished using such special abrasive operations as finishing grinding, superfinishing or belt grinding [1],[3]. Relatively new trend emerging recently in the industry is to improve the machinability of hard steel materials using special ball and sliding burnishing tooling.

As reported by Klocke *et al.* [4] the Ra parameter after burnishing of bearing steel of 62 HRC hardness was reduced from initial  $Ra=0.3 \mu\text{m}$  to below  $Rab=0.17 \mu\text{m}$  and the compressive residual stresses of -1600 MPa were induced into the surface layer. Similarly [5], after burnishing of a hardened steel component (64 HRC) using a ceramic ball of 6.35 mm diameter, the roughness  $Ra=0.2 \mu\text{m}$  and the ratio of  $Ra/Rab$  ranged from 1.4 to 2.4. This technology is also effective in improving the final quality of the previously ball-end milled surfaces of dies and moulds using CNC machining centers [6]. This innovative non-removal machining technique was also examined in this study taking into consideration both surface finish and microstructure alterations in the subsurface layer.

---

<sup>1</sup> Faculty of Mechanical Engineering, Opole University of Technology, 5 Mikołajczyka Street, Opole 45-271, Poland

## 2. EXPERIMENTAL DETAILS

### 2.1. CHARACTERIZATION OF MACHINING SYSTEM AND MACHINING CONDITIONS

In this investigation, hard machining trials (Fig. 1b) were performed on the specimens made of 41Cr4 (AISI 5140) steel with Rockwell's hardness of  $57\pm 1$  HRC. Low content CBN tools containing about 60% CBN, grade CB7015 by Sandvik Coromant, were used. Hard turning conditions were as follows: cutting speed of 150 m/min, variable feed rate of 0.075 (HT1), 0.1 (HT2) and 0.125 (HT3) mm/rev, depth of cut of 0.15 mm/rev.

Roller burnishing was performed under static ball-workpiece interaction using special burnishing tool equipped with  $\text{Si}_3\text{N}_4$  ceramic ball of 12 mm diameter and controlled spring-based pressure system to generate desired load, as shown in Fig. 1c. The burnishing head was mounted in the turret (1) and it was additionally included into CNC program along with CBN turning. Burnishing conditions were as follows: burnishing speed of 25 m/min, burnishing feed  $f_b$  of 0.05 mm/rev (HT1+B1), 0.075 mm/rev (HT2+B2) and 0.1 mm/rev (HT3+B3), which was always lower than turning feed  $f_t$  and the tool correction of 0.25 mm in the CNC control system. Both hard turning (HT) and ball burnishing (BB) operations were performed on a CNC turning center, Okuma Genos L200E-M (Fig. 1a).

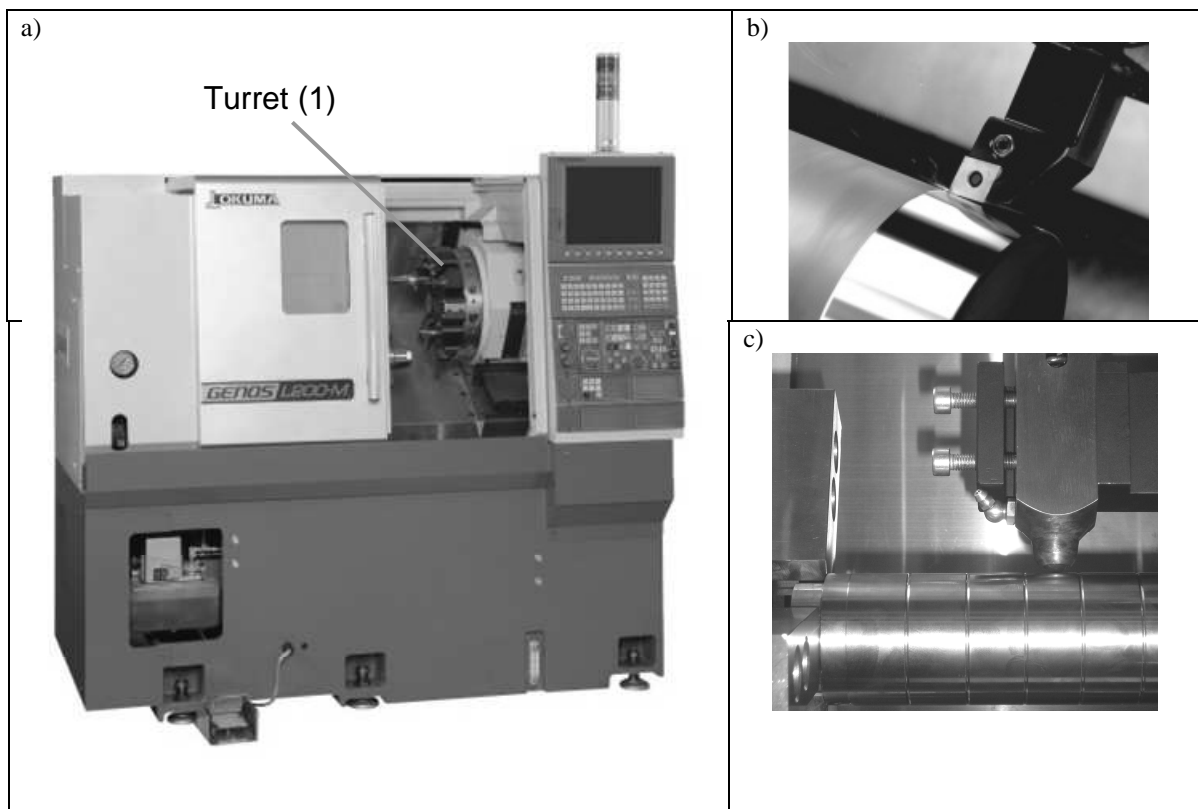


Fig. 1. CNC turning center, (a) used to perform sequential dry hard turning, (b) and ball burnishing, (c) operations

## 2.2. MEASUREMENTS OF SURFACE INTEGRITY

Surface profiles/ topographies were recorded and 2D and 3D roughness parameters were estimated on the scanned areas of 2.4 mm×2.4 mm by means of a TOPO-01P profilometer with a diamond stylus radius of 2 μm (Fig. 3).

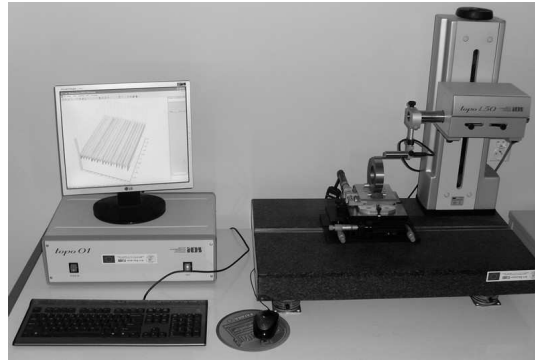


Fig. 2. 3D profilometer, model TOPO 01P

Micro-hardness ( $\mu\text{HV}$ ) of the machined and polished samples across the subsurface was measured using a LECO hardness tester MHT Series 200 with a Berkovich indenter at a load of 50 G, i.e. HV0.05. A hardness variation within subsurface layer of about 100 μm thickness was determined. In order to avoid interference of indentations and increase the measuring accuracy ( $h_i=l_i \times \sin \alpha$ ), the measurements were performed on the inclined sections, inclined at about  $3^\circ$  to the outer surface (see detail in Fig. 10). Based on the micro-hardness data the material hardening rates related to the maximum values of microhardness in the subsurface layer were determined.

The microstructure and texture changes induced by burnishing were examined by means of a scanning microscope, model HITACHI S-3400N equipped with X-ray diffraction head EDS, model THEMO NORAN System Six. Both SEM and BSE images were recorded. These analyses were performed on mechanically and chemically polished sections.

## 3. EXPERIMENTAL RESULTS AND DISCUSSION

### 3.1. GEOMETRICAL FEATURES OF TURNED SURFACES

In general, the hard turned surfaces have specific geometrical features depending on the initial hardness of the workpiece and machining conditions used. In addition, ball burnishing of the hardened workpiece changes the mechanical properties and results in the generation conditions of both the surface and subsurface layer. Figures 3-9 presents integrally the geometrical state of the surfaces produced by (HT+BB) sequential process.

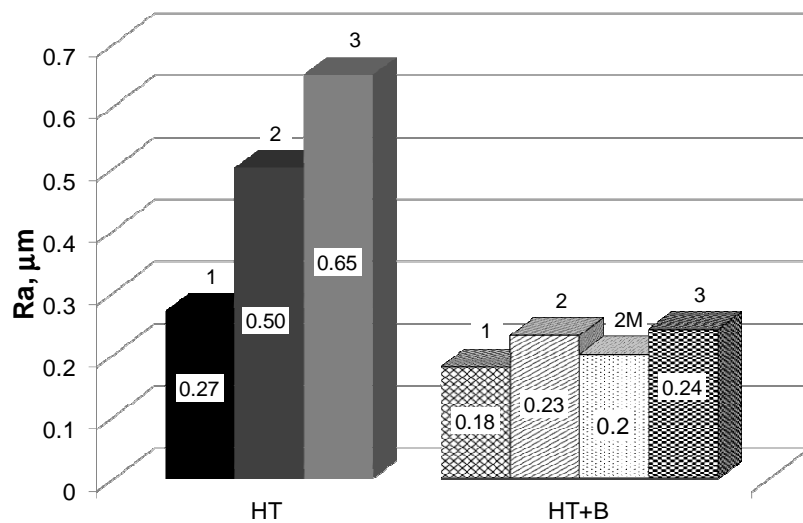


Fig. 3. Comparison of Ra roughness parameters for hard turned and burnished surfaces

Figure 3 presents the obtained values of the Ra parameter with different feeds. First, dry hard operations cause that Ra parameter diminishes but this effect is more pronounced for the lowest feed rate of 0.075 mm/rev applied for which the minimum value of  $Ra=0.27 \mu\text{m}$  was obtained (variant HT1). The second observation is that the Ra parameter decreases due to burnishing action and for all process variants its value is about  $0.2 \mu\text{m}$ . Of course the ratio of  $Ra_t/Ra_b$  depends distinctly on the initial roughness generated in CBN hard machining. The Rz parameter and fractions of Rp and Rv components within the total height Rz depend not only on the feed value but the process variant. As can be seen in Fig. 4 the values of Rz parameter obtained after ball burnishing are about 20-50 % lower than for initial dry HT operations. The greatest effects were achieved for initial hard surfaces turned with lower feeds. It should be noted in Fig. 4 that burnishing causes that the peak heights are substantially reduced, as also depicted in appropriate cases in Fig. 5

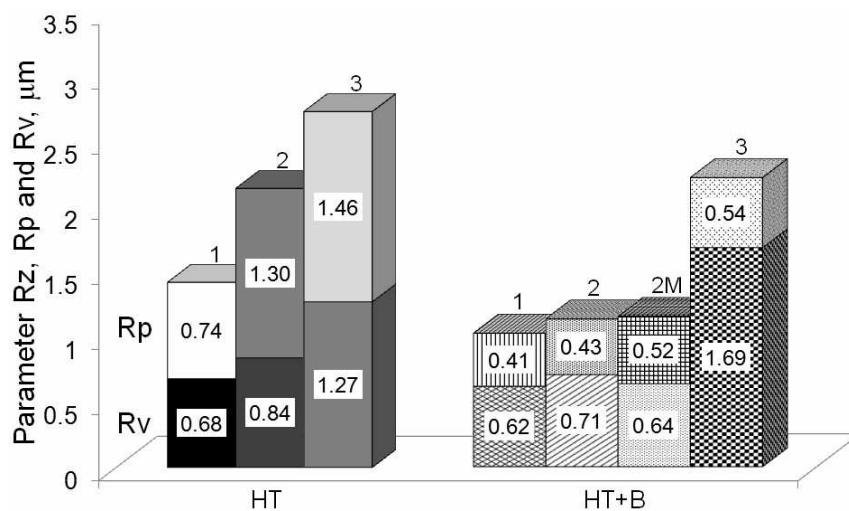


Fig. 4. Comparison of Rz roughness parameters for hard turned and burnished surfaces

As can be seen in Fig. 5 dry hard turning produced surface profiles with very sharp and regular tool nose traces, for which the  $R_{sm}$  parameters are almost equal to the feed value, with very small slopes  $R_{\Delta q}$ , generally not greater than  $2^0$ . Oppositely, BB produced profiles with lower blunted peaks, as it was documented in Figs. 5b1-b3. This effect results partly from both plastic deformation and spalling (brittle fracture) of the hard micro-regularities, which mostly appears in the case HT3+B3 (Fig. 5b3). As a result, the regularity of the profile is disturbed visibly, especially for the highest feed rate  $f_b$  employed.

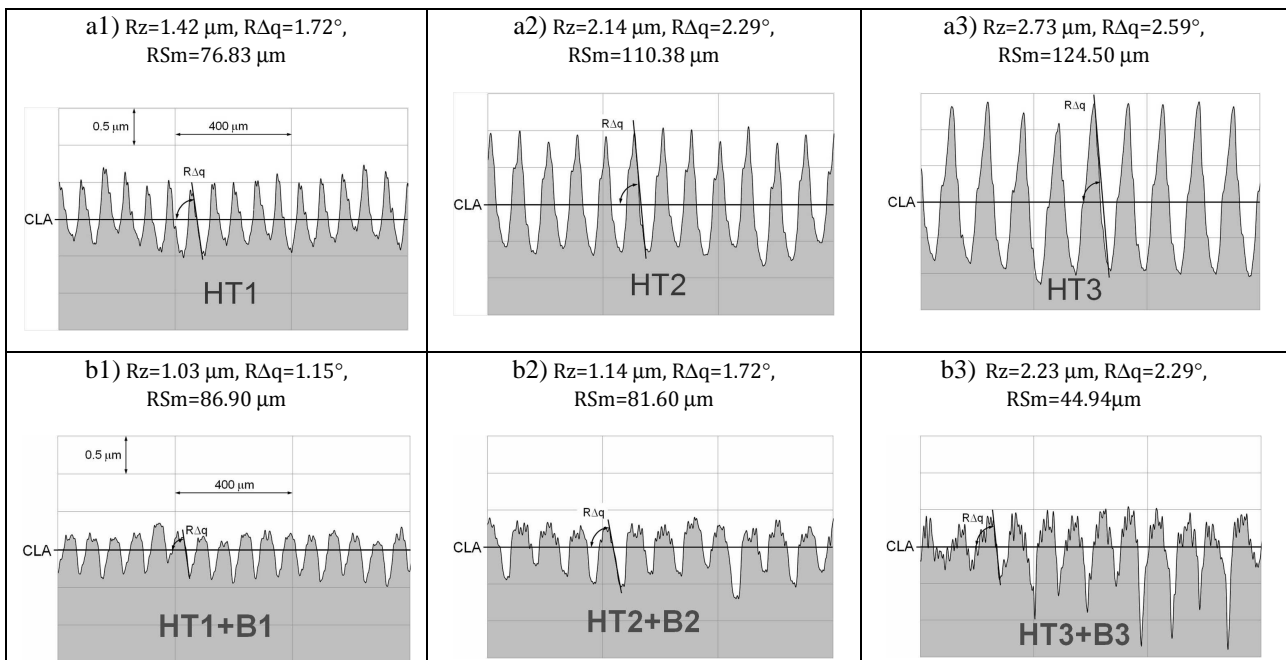


Fig. 5. Examples of surface profiles produced in dry hard turning: (a1-a3) and burnishing (b1- b3) with variable feeds

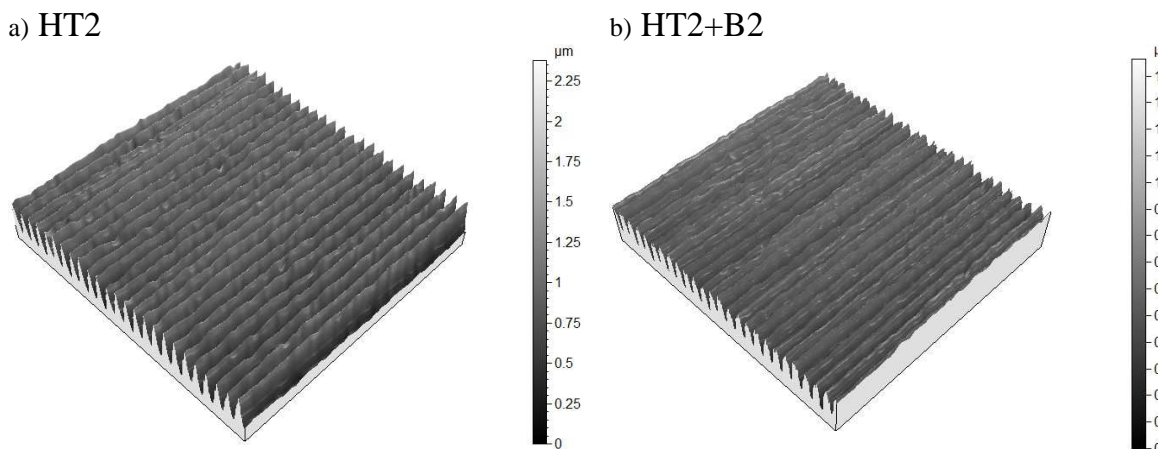


Fig. 6. Surface topographies produced: a), in dry hard turning, b) in dry hard turning and burnishing

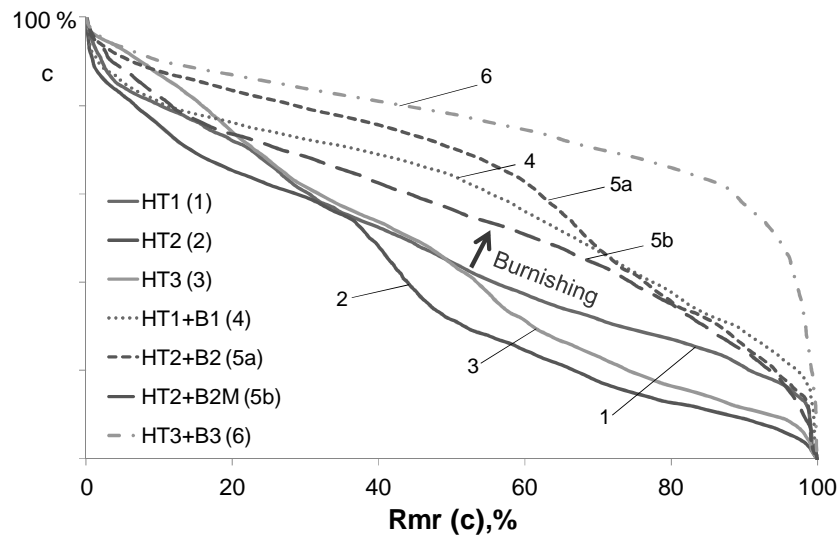


Fig. 7. Material ratio curves for dry hard turning (HT) and burnishing (HT+B) operations with variable feeds

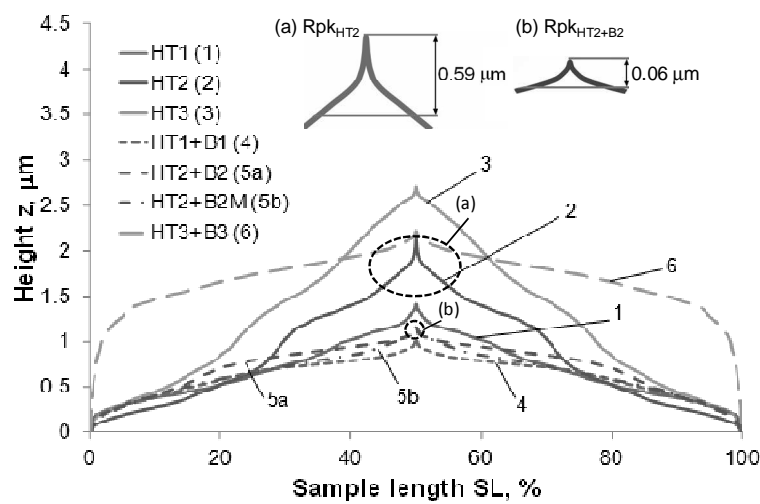


Fig. 8. Family of SCGC's for hard turned and burnished surfaces

Fig. 7 confirms that CBN hard turning produces profiles with unsatisfactory bearing properties. As depicted in Fig. 7 the BAC's are linear or degressive as produced mainly by dry hard operations (cases 1 and 2). On the other hand, the material ratio increases progressively after ball burnishing as represented by BAC's # 4, 5 and 6. The differences in the bearing properties of surface profiles produced can be visibly represented in the form of SCGC (symmetric curve of geometrical contact) curves shown in Fig. 8 and in Rku-Rsk plot shown in Fig. 9. It can be seen in Fig. 8 that only after hard turning surface profiles with positive skewness are produced but the profile with small value of Rpk was generated in the case HT1. Moreover, the effect of burnishing is to decrease the values of the reduced peak height Rpk from initial values of 0.25-0.85  $\mu\text{m}$  to 0.06-0.10  $\mu\text{m}$ . Such modification of the profile peaks implies distinctly shorter running-in periods during part service.

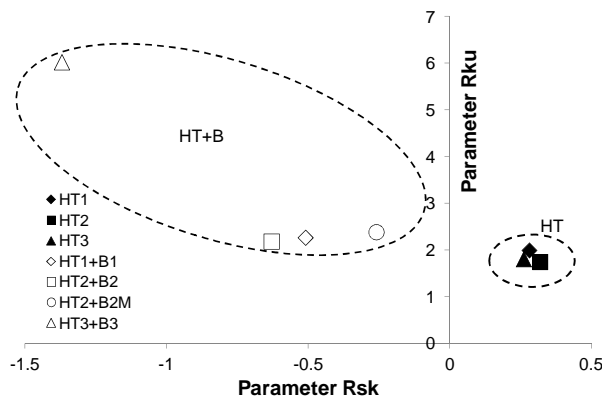


Fig. 9. Kurtosis vs skewness map for a range of hard turning and burnishing operations

Two characteristic areas with different pairs of Rku and Rsk parameters can be distinguished in Fig. 9. Correspondingly to curves # 4, 5 and 6 negative values of the skewness were determined, namely  $Rsk = -0.51, -0.63$  and  $-1.37$ . These Rsk values suggest that surface profiles generated by sequential CBN turning and ball burnishing processes have better bearing properties. Otherwise, surfaces with sharp irregularities produced by dry hard turning have better locking properties. In addition, kurtosis near 2 means that the profiles are congregated at the extremes (they are described in tribology as platykurtic).

Worse bearing properties of surfaces generated by hard turning in comparison to those obtained after ball burnishing can also be related to lower values of upper material ratio  $Mr1$ . For the three feed rates used they are equal to:  $Mr1^{HT}/Mr1^{BB} = 20.67\% \text{ vs. } 6.30\%, 33.67\% \text{ vs. } 3.98\%.$  and  $24.77\% \text{ vs. } 5.54\%$

### 3.2. MICROHARDNESS AND THERMAL EFFECTS

Distribution of microhardness in the subsurface layer at the distance of  $100 \mu\text{m}$  from the surface depends on the variant of cryogenically assisted process, as exemplarily shown in Fig. 10. Dry hard turning causes that maximum microhardness is localized close to the

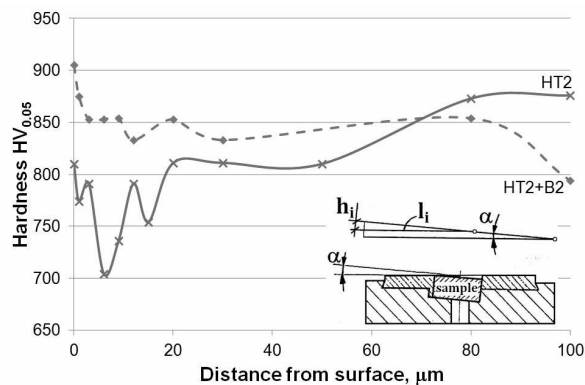


Fig. 10. Microhardness distributions for hard turning (HT) and sequential (HT+BB) operations ( $f_b=0.1 \text{ mm/rev}$ )

surface whereas for cryogenic cooling the trend is to shift this point beneath the surface (12-15  $\mu\text{m}$ ). As a result, after dry hard turning maximum microhardness HV0.05 measured directly underneath the generated surface was about 800 MPa. After ball burnishing the sublayer is hardened and in consequence microhardness in the zone adjacent to the surface increases to about 900 MPa.

### 3.3. MICROSTRUCTURAL ALTERATIONS OF THE SURFACE LAYER

As mentioned above, quantitative microstructural analysis was performed using SEM/BSE technique with additional phase content measurements using EDS technique. The second technique allows to determine the chemical composition of the surface layer and identify the structural effects due to intensive heating and plastic deformation. Samples, which were mounted in conductive resin, were prepared by mechanical grinding, diamond polishing and electropolishing. Fig. 11 shows an exemplary BSE image of the bulk material before burnishing with characteristic microstructure consisting of untempered martensite.

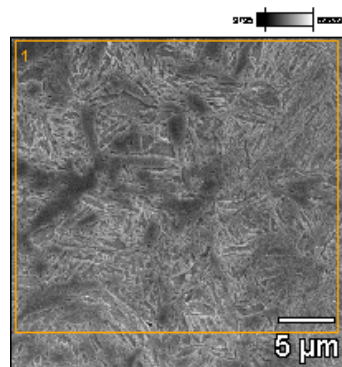


Image name: HT2  
Accelerating voltage: 15.0 kV  
Magnification: 4000 $\times$   
Microstructure: untempered martensite

Fig. 11. BSE image showing microstructure for 41Cr4 steel core after quenching

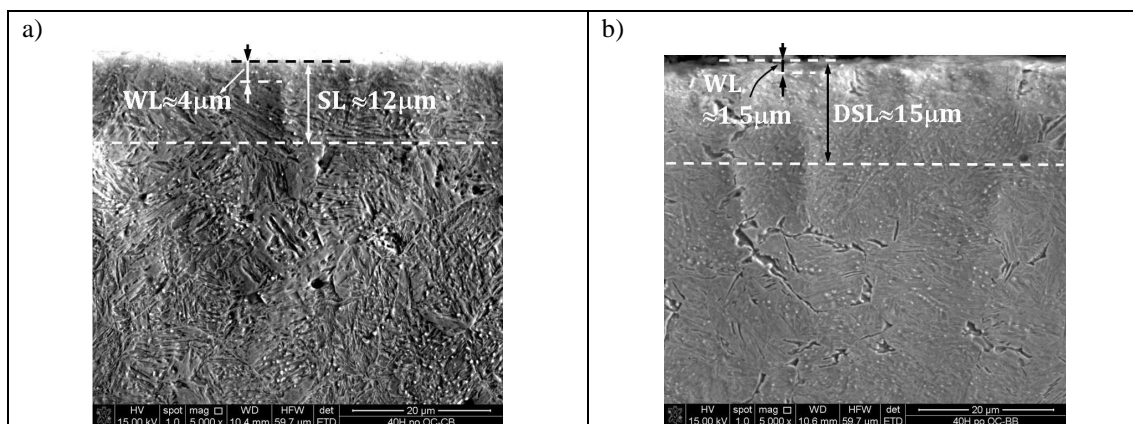


Fig. 12. Microstructures of the surface layer after: (a) dry hard machining (HT2), (b) sequential hard machining (HT2) and ball burnishing (B2). Magnification  $\times 5000$

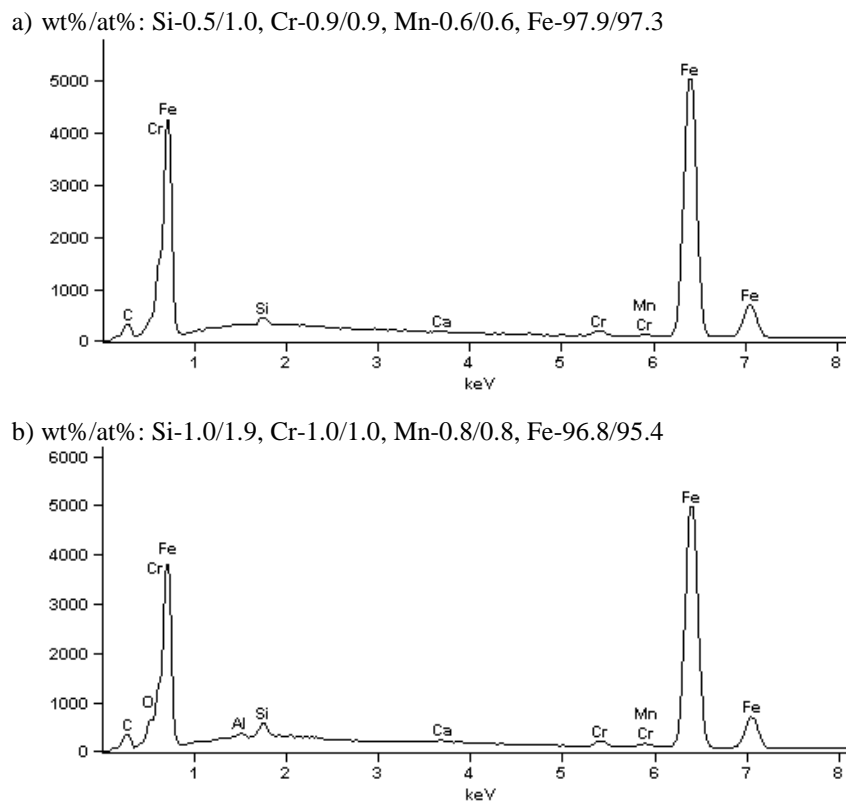


Fig. 13. EDS spectra of the surface layer after: (a) dry hard turning (HT2) and (b) sequential (HT2+B2) machining

Fig. 12 shows BSE microphotographs of surface layer (SL) produced by dry hard turning (Fig. 12a) and additional ball burnishing (Fig. 12b) operations. It should be noted that the width of surface layer coincides well with microhardness distribution presented in Fig. 10. The BSE images confirm that ball burnishing causes that the thickness of the white layer (WL) is visibly diminished, from 4  $\mu\text{m}$  to 1.5  $\mu\text{m}$  due to plastic deformation of profile peaks (Fig. 12b). On the other hand, BB produced a highly deformed structure pronounced by visibly elongated grains with submicron dispersive carbides. In particular, in this case, easily noticed severely deformed surface layer (DSL) of about 15  $\mu\text{m}$  thickness is observed. This image also shows martensite structure with the grain boundaries of retained austenite.

No evidence of a chemically modified surface layer was observed within the subsurface layer as documented by relevant EDS spectra presented in Fig. 13. The contents of alloying elements correspond to data provided by steel manufacturers and metallurgists.

#### 4. CONCLUSIONS

The following conclusions can be drawn from this study :

1. Ball burnishing of the hard workpiece results in substantial modifications of both surface and surface layer.

2. Dry hard turning produced surface profiles with regular tool nose traces and lower surface roughness. The minimum value of  $R_a=0.27 \mu\text{m}$  (correspondingly  $R_z=1.42 \mu\text{m}$ ) was obtained for the turning feed of 0.075 mm/rev and burnishing. For BB process with the feed of 0.05 mm/rev its value decreased below  $0.2 \mu\text{m}$  ( $R_z$  about  $1 \mu\text{m}$  typical for precision hard machining).

3. Surfaces produced by sequential (HT+BB) machining process are distinctly flattened causing better bearing properties, correspondingly to negative values of  $R_{sk}$  parameter. On the other hand, surfaces generated by dry hard turning consist of very sharp irregularities and  $R_{sk}$  is always positive in the range of 0.3.

4. Subsurface layers produced by sequential (HT+BB) consist of thinner white layer. This effect corresponds to higher microhardness readings of about  $900 \text{HV}_{0.05}$  near the surface. In contrast, for dry hard turning measured microhardness value is about  $820 \text{HV}_{0.05}$ .

5. SEM examinations of the SL revealed the presence of martensite structure with the grain boundaries of retained austenite. On the other hand, sequential HT+BB machining produced a significantly finer crystalline structure with submicron dispersive carbides.

#### REFERENCES

- [1] GRZESIK W., 2008, *Advanced Machining Processes of Metallic Materials*. Elsevier, Amsterdam.
- [2] KLOCKE F., BRINKSMEIER E., WEINERT K., 2005, *Capability profile of hard cutting and grinding processes*, Annals of the CIRP, 54/2/557-580.
- [3] GRZESIK W., ŽAK K., 2012, *Modification of surface finish produced by hard turning using superfinishing and burnishing operations*, J. Mater. Proc. Technol, 212/315-322.
- [4] KLOCKE F., LIERMAN J., 1998, *Roller burnishing of hard turned surfaces*, Int. J. Mach. Tools Manuf. 38,419-423.
- [5] LUCA L., NEAGU-VENTZEL S., MARINESCU I., 2005, *Effects of working parameters on surface finish in ball-burnishing of hardened steels*, Prec. Eng., 29/253-256.
- [6] LÓPEZ DE LACALLE L.N., LAMIKIZ A., MUNOJA J., SÁNCHEZ J.A., 2005, *Quality improvement of ball-end milled sculptured surfaces by ball burnishing*, Int. J. Mach. Tools Manuf., 45/1659-1668.